Journal of Energy Technology

JET Volume 8 (2015) p.p. 51-62
Issue 1, September 2015

www.fe.um.si/en/jet.html

NUMERICAL ANALYSIS OF A HEAT EXCHANGER: ANSYS VS SOLIDWORKS

NUMERIČNA ANALIZA TOPLOTNEGA PRENOSNIKA: ANSYS IN SOLIDWORKS

Marko Pezdevšek[ℜ], Igor Spaseski, Igor Ščuri, Matej Fike, Gorazd Hren

Keywords: numerical analysis, heat exchanger, Ansys CFX, SolidWorks

Abstract

In this article, three-dimensional numerical analyses are presented with the goal of investigating heat transfer and fluid flow characteristics of an un-baffled shell-and-tube heat exchanger, using Ansys CFX and SolidWorks Flow Simulation software packages. The analyses of the overall heat transfer coefficient and pressure drop values inside the shell and tubes were performed on designed meshes with similar number of elements, for various Reynolds numbers. All numerically obtained results were validated with experimental measurements from literature.

Povzetek

V članku so predstavljeni rezultati in izvedba tridimenzionalnih numeričnih analiz prenosa toplote za primer cevno paketnega prenosnika toplote. Za izvedbo numeričnih simulacij sta bila uporabljena programska paketa Ansys CFX ter SolidWorks Flow Simulation. Analiza skupnega koeficienta prenosa toplote ter tlačnih padcev v ceveh in plašču je bila izvedena s strukturirano mrežo za več Reynoldsovih števil. Z namenom, da ovrednotimo rezultate numeričnih simulacij, smo le te primerjali z eksperimentalno pridobljenimi vrednostmi iz literature.

ℜ Corresponding author: Marko Pezdevšek, Tel.: +386 70 741 069, Mailing address: Vodovodna ulica 9, 1433 Radeče, Slovenia, E-mail address: m.pezdevsek@gmail.com

1 INTRODUCTION

Heat exchangers are one of the most commonly used pieces of equipment in numerous mechanical industries and home appliances. They are used to transfer heat between two process streams in various processes that involve cooling, heating, condensation, boiling and evaporation. Different heat exchangers are named according to their applications. For instance, heat exchangers being used to boil are known as boilers, while heat exchangers for condensation purposes are called condensers.

Heat exchangers are available in many configurations and are classified according to their application, process fluids, or mode of heat transfer and flow. They can also be classified based on shell and tube passes, types of baffles, arrangement of tubes, and whether they have smooth or baffled surfaces. Heat exchangers can transfer heat through convection or conduction. There are two primary flow arrangements in the heat exchanger: a parallel-flow and a counter-flow. Two fluids flow from the same end to another end in a parallel flow heat exchanger. For the counter-flow arrangement, the two fluids run in the opposite direction from two ends of the heat exchanger. The selection of a particular heat exchanger configuration depends on several factors, which may include the area requirements, maintenance, flow rates and fluid phase, [1].

Shell-and-tube heat exchangers (STHE) consist of a bundle of tubes enclosed within a cylindrical shell. Two fluids, of different starting temperatures, flow through the heat exchanger. One fluid flows through the tubes and the other flows outside the tubes but inside the shell. Heat is transferred from one fluid to the other through the tube walls, either from tube side to shell side or vice versa. The fluids can be either liquids or gases on either the shell or the tube side. Most commonly used STHE have large heat transfer surface area-to-volume ratios to provide increased heat transfer efficiency. Shell and tube heat exchangers are simple to manufacture for a large variety of sizes and flow configurations and can operate at high pressures and high temperatures. The STHE can be employed for processes that require large quantities of fluid to be heated or cooled. They are easy to clean and repair in case of malfunction and offer greater flexibility of mechanical features to withstand any service requirement, [2].

The performance and efficiency of heat exchangers are measured through the amount of heat being transferred using the area of heat transfer and the pressure drop. Its efficiency is usually defined with an overall heat transfer (HT) coefficient, [1]. Thus, in order to calculate these parameters, the flow distribution and temperature fields inside the shell and tubes must be obtained. For this reason, several CFD (computational fluid dynamics) flow simulations of simple un-baffled STHE are carried out, using the Ansys CFX and SolidWorks Flow Simulation (SWFS) software packages and compared to experimental data from literature, [1].

2 GOALS

With the aim of investigating the difference between used numerical software packages, three-dimensional CFD simulations were carried out to obtain counter-current STHE global parameters. The difference of the software packages' purposes and limitations must be emphasized. Ansys CFX is a well-known commercial standalone CFD software for numerical analyses, while SolidWorks Flow Simulation is a part of CAD (computer-aided design) package.

The geometry of the heat exchanger was modelled in SolidWorks (SW). We created corresponding meshes in SWFS and in ICEM CFD software. Simulations were carried out in order to resolve the heat transfer coefficient and pressure drop characteristics of the heat exchanger for different Reynolds numbers ranging from $9.2 \cdot 10^4$ to $15.2 \cdot 10^4$ for the shell and from $2.16 \cdot 10^4$ to $3.6 \cdot 10^4$ for tubes. The designed meshes with associated boundary conditions were iteratively solved with steady-state solvers using different turbulence models. In order to validate the numerically obtained results, we compared them to existing experimental measurements from literature, [1].

3 NUMERICAL APPROACH

The heat exchanger numerical model was simulated assuming steady-state conditions, using conventional Reynolds averaged Navier-Stokes (RANS) turbulence models. In general, for modelling the turbulent flow and heat transfer processes, two equation models are most commonly used, [1]. SWFS provides only the k-ε turbulence model, while Ansys CFX offers various choices. In order to obtain the most suitable turbulence model, multiple test calculations were carried out and obtained results were compared with experimental measurements from literature. The model that most accurately predicts the results was used for further calculations.

3.1 Geometry

The three-dimensional STHE geometry was designed in the SW software package in accordance with the prescribed dimensions from [1]. The geometry consisted of four main parts: shell, inlet tube, outlet tube and nineteen inner tubes. Table 1 presents description and dimensions of the STHE geometry in millimetres.

Table 1: *Dimensions of the heat exchanger geometry.*

Description	Value [mm]
Overall dimensions	54 × 378 × 5850
Shell diameter	108
Tube outer diameter	16
Tube inner diameter	14.6
Shell/tube length	5850
Inlet tube length	70
Outlet tube length	200

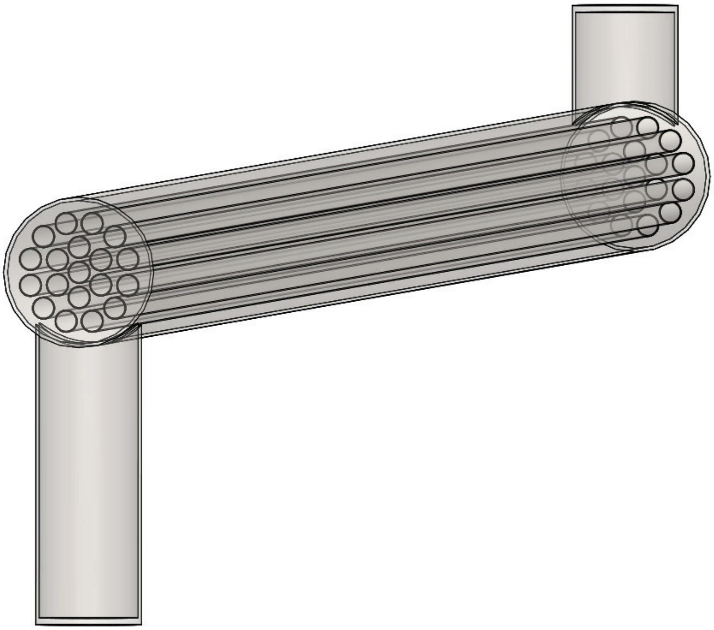

Figure 1: *Heat exchanger model.*

3.2 Numerical mesh

In CFD, the numerical mesh has two elementary functions: first, definition of the modelled geometry; second, discretization of the computational domain. The constructed mesh has to describe the physical geometry of the modelled object. The complexity of the modelled object affects the final mesh size and consequently the required design time. The amount of computer resources needed for the calculation of numerical simulations is proportional to the mesh intersection density and longitudinal resolution. The accuracy for solving the governing equations is dependent on the number of discrete elements and nodes of the mesh. Generally, a numerical solution becomes more accurate when a mesh with a greater resolution is used. Furthermore, a mesh with smaller element size is usually used in regions where high temperature and pressure gradients of critical quantities are occurring. In numerical simulations, we have to balance accuracy with the limitations of computer resources.

Structural computational meshes for fluid and solid domains of the shell, inlet tube, outlet tube, and inner tubes were designed with a pre-processor ICEM CFD for the analysis in Ansys CFX software. Once the partial volume meshes are created, they were merged in Ansys CFX to represents the full computational domain. In SW, the mesh was designed with an in-built mesh manager in SWFS software package for the modelled domain.

3.2.1 SolidWorks Flow Simulation

In order to acquire grid-independent results, several test calculations of the pressure drop in the shell and tubes, as well as the HT coefficient, were performed in SWFS. Three meshes with different number of elements were designed and used for performing simulations at inlet velocities of 1.2 m/s for the shell and 1.8 m/s for tubes with the corresponding boundary conditions described in Chapter 3.3. The deviation between numerically obtained results and experimental values from [1] is presented in Table 2.

Table 2: *Deviation between numerically obtained results and experimental values for different mesh resolutions.*

Mesh resolution (approx. number of elements)	Coarse (2,000,000)	Medium (3,500,000)	Fine (5,000,000)
Pressure drop deviation in shell [%]	-22.34	-17.90	-16.32
Pressure drop deviation in tubes [%]	5.66	4.27	5.51
Overall HT coefficient deviation [%]	-14.23	-9.20	-8.85

From Table 2, it is evident that the calculation results do not deviate remarkably between the medium and fine mesh. From that, it can be concluded that the mesh density does not significantly affect the calculation results in this case and the medium-sized mesh was used as a reference for further simulations in SWFS as optimal mesh density.

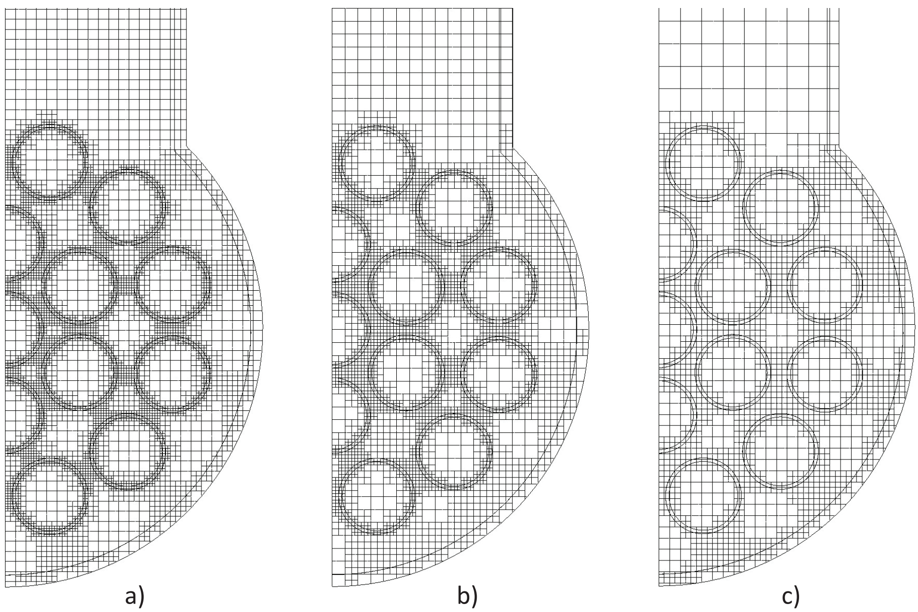

Figure 2: *Mesh resolutions a) course, b) medium and c) fine.*

3.2.2 ICEM CFD

As the reference mesh for computation in SW had approximately 3.5 million elements, we decided to design a mesh with comparable number of elements in ICEM CFD for the analysis in Ansys CFX.

A dimensionless wall distance (y^+) value plays an important role in turbulence modelling for the near wall treatment. In order to resolve the boundary layer sufficiently, inflation on the walls was created and y^+ simulations were calculated. Precise computed results were possible only if the resolution of the mesh near the walls satisfied the condition $y^+ < 1$.

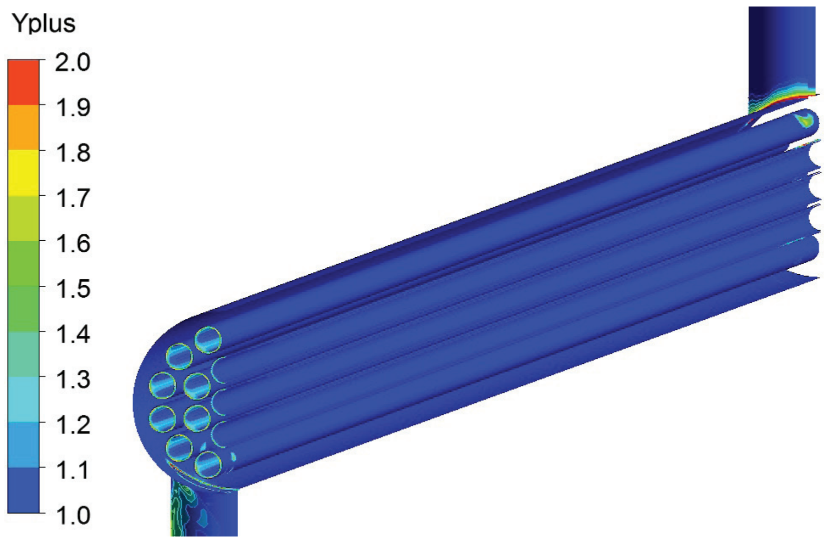

Figure 3: *y^+ value for the shell Reynolds number $13.68 \cdot 10^4$.*

Different turbulence models available in Ansys CFX were evaluated to investigate their application for our case. As seen in Table 3, the overall HT coefficient and pressure drop obtained from these models were compared (in %) to the experimental results [1].

Table 3: *Turbulence model comparison of overall HT coefficient and pressure drop.*

Turbulence model	SST	*k-ω*	*k-ε*	RNG *k-ε*
Pressure drop in shell deviation [%]	-1.57	-3.30	19.32	21.24
Pressure drop in tubes deviation [%]	-14.54	-20.87	-8.98	-0.06
Overall HT coefficient deviation [%]	-0.20	-1.85	14.54	15.14

Based on the results in Table 3, the SST model was chosen for further analysis.

In Figure 4, the designed meshes are shown, which clearly represent different types of mesh creation. A Cartesian-based mesh generated in SWFS, [3], and a typical structured mesh designed in ICEM CFD are presented.

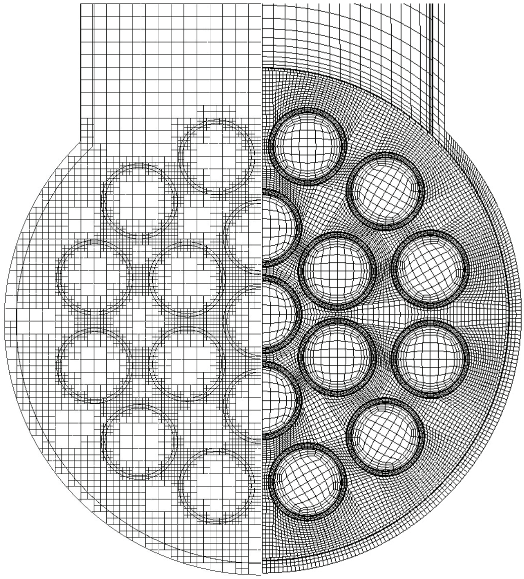

Figure 4: *Designed meshes in SWFS (left) and in ICEM CFD (right) used for analysis.*

As seen in Figure 4, the number of elements seems greater in ICEM CFD than in SWFS. SWFS only provides Cartesian-based mesh generation [3], which, when refinement is used, splits an element in half along all three coordinate axis (an element cannot be split in only one axis). Thus, where the mesh refinement is used, there are up to four times more elements along the length of the model in SWFS than in ICEM CFD. Therefore, it is difficult to achieve the same number of elements in the longitudinal direction.

3.3 Boundary conditions and convergence criteria

For achieving good correlation with experimental results, precise boundary conditions needed to be applied to the model.

The shell inlet was defined as a velocity inlet with an initial temperature of 317 K. The tube inlet was also defined as a velocity inlet with an initial temperature of 298 K. Outlets for both shell and tube were defined as pressure outlets with atmospheric pressure. The outer walls were set as adiabatic. The tube walls were set for transferring of heat between the shell and tube side fluids. The symmetry boundary condition was applied for both software packages.

To satisfy the convergence criteria, the residual type was set to root mean square (RMS) with the target value of $1 \cdot 10^{-5}$. We also set the number of maximum iterations to 500 and automatic timescale control. Both software packages have an automatic system for stopping the analysis when it reaches the defined convergence criteria. In Ansys, we encountered a problem with convergence, so we inserted monitor points to monitor the desired parameters. The simulation was stopped when the selected parameters ceased altering their values.

4 RESULTS

4.1 Pressure drop

Pressure drop values at different Reynolds numbers were acquired from both software packages and calculated directly from CFD results. These results were compared with available experimental data from [1] and are presented in Table 4 and Table 5, respectively.

Table 4: *CFD and experimental results of pressure drop [1].*

Reynolds number [$\cdot 10^4$]		Ansys SST model Pressure drop [kPa]		SolidWorks Pressure drop [kPa]		Experimental Pressure drop [kPa]	
Shell	Tube	Shell	Tube	Shell	Tube	Shell	Tube
9.20	2.16	5.28	7.74	4.37	6.89	5.60	6.60
10.64	2.52	6.96	10.02	5.74	9.01	7.20	8.70
12.16	2.88	8.85	12.56	7.25	11.37	8.90	10.90
13.68	3.24	10.97	15.35	8.87	13.97	10.80	13.40
15.20	3.60	13.26	18.37	10.71	16.81	12.80	16.10

Table 5: *Deviation between CFD and experimental results of pressure drop.*

Reynolds number [$\cdot 10^4$]		Ansys SST model Pressure drop deviation [%]		SolidWorks Pressure drop deviation [%]	
Shell	Tube	Shell	Tube	Shell	Tube
9.20	2.16	-5.70	17.32	-21.98	4.38
10.64	2.52	-3.37	15.22	-20.32	3.53
12.16	2.88	-0.51	15.23	-18.54	4.31
13.68	3.24	1.57	14.54	-17.90	4.27
15.20	3.60	3.62	14.11	-16.33	4.42

The pressure drop in shell is under-predicted by SW with a deviation of 16–22%, whereas the pressure drop in tubes is over-predicted by approximately 4%. In Ansys CFX, the pressure drop in the shell is under-predicted with a deviation of 1–6%. The deviation in tubes is over-predicted by 14–17%. Generally, Ansys better predicts the pressure drop in the shell by 16%, while SW computed better results for the tube pressure drop by about 11%, as presented in Table 5 and presented as graphs in Figure 5.

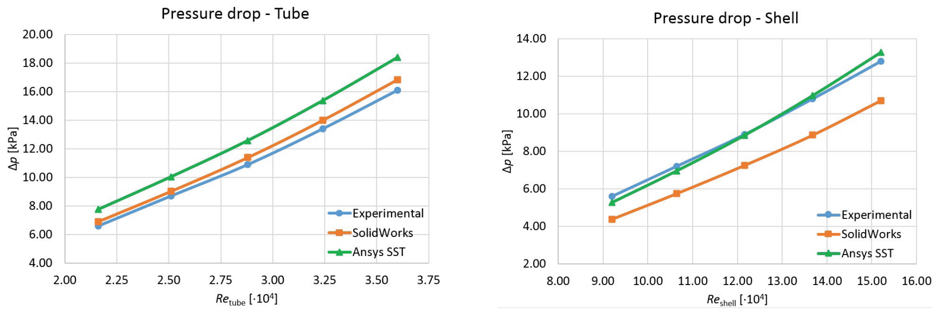

a) b)

***Figure 5:** Comparison of pressure drop on a) shell side and b) tube side.*

4.2 Overall heat transfer coefficient

From numerical simulations, we acquired heat transfer rate values and temperatures from which we calculated the overall heat transfer coefficient U with equation:

$$U = \frac{\dot{Q}}{A \cdot \Delta T_{\mathrm{LM}}}, \tag{4.1}$$

where:

$\dot{Q}$ - heat transfer rate;

A - heat transfer surface area;

ΔT_{LM} - logarithmic mean temperature difference.

The logarithmic mean temperature difference ΔT_{LM} or LMTD is calculated to estimate the average temperature difference throughout the heat exchanger. It's defined with equation:

$$\Delta T_{\mathrm{LM}} = \frac{\Delta T_1 - \Delta T_2}{\ln\left(\frac{\Delta T_1}{\Delta T_2}\right)}, \tag{4.2}$$

where:

ΔT_1, ΔT_2 - the temperature difference between the two streams.

For counter-current flow in the shell and tube heat exchangers, the temperature difference is defined with $\Delta T_1 = T_{\mathrm{Hot\_In}} - T_{\mathrm{Cold\_Out}}$ and $\Delta T_2 = T_{\mathrm{Hot\_Out}} - T_{\mathrm{Cold\_In}}$. The inlet temperature for the shell was set to $T_{\mathrm{Hot\_In}}$=317 K and for tubes to $T_{\mathrm{Cold\_In}}$=298 K. The temperatures $T_{\mathrm{Cold\_Out}}$ and $T_{\mathrm{Hot\_Out}}$ were numerically obtained.

Table 6: *CFD and experimental results of an overall HT coefficient [1].*

Reynolds number [·10⁴]		Ansys SST model	SolidWorks	Experimental
Shell	Tube	Overall HT coefficient [W/m²·K]	Overall HT coefficient [W/m²·K]	Overall HT coefficient [W/m²·K]
9.20	2.16	1847	1785	1965
10.64	2.52	2114	1997	2196
12.16	2.88	2367	2195	2414
13.68	3.24	2626	2375	2621
15.20	3.60	2879	2548	2819

Table 7: *Deviation between CFD and experimental results of an overall HT coefficient.*

Reynolds number [·10⁴]		Ansys SST model	SolidWorks
Shell	Tube	Overall HT coefficient deviation [%]	Overall HT coefficient deviation [%]
9.20	2.16	-5.99	-9.18
10.64	2.52	-3.75	-9.05
12.16	2.88	-1.96	-9.07
13.68	3.24	0.20	-9.38
15.20	3.60	2.14	-9.63

The overall HT coefficient is under-predicted by SW by approximately 9%. In Ansys CFX, the overall HT coefficient is under-predicted with a deviation of 1–6%. Generally, the Ansys SST turbulence model better predicts the overall HT coefficient by 4–8%, as seen in Table 7 and Figure 6.

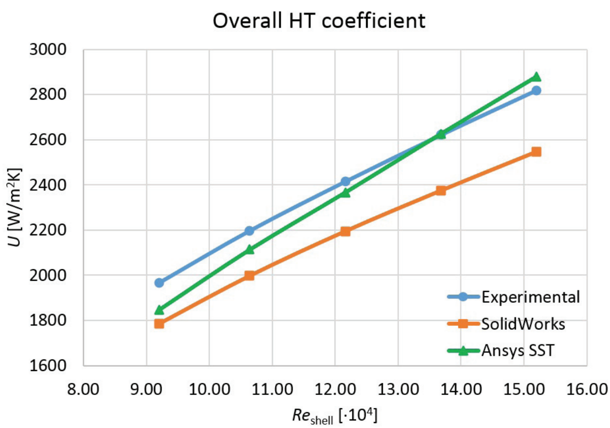

Figure 6: *Comparison of overall heat transfer coefficient.*

5 CONCLUSIONS

Simulations of the shell-and-tube heat exchanger global parameters for various Reynolds numbers were made in order to compare the results from different software packages and then validate them with experimental data as a reference.

For this CFD study, numerical meshes for the geometry seen in Figure 1 were designed. Grid independence was studied with three meshes designed in SWFS, comprised of different numbers of elements (Table 2) with corresponding boundary conditions. Based on the results, the medium-sized mesh has been recognised as suitable and was chosen for further analyses. A mesh with a comparable number of elements was designed in ICEM CFD for the analysis in Ansys CFX. In the process of the mesh design, a dimensionless wall distance (y^+) value was considered.

Different turbulence models were available and evaluated to investigate their application for this case. The tested turbulence models were SST, *k-ω, k-ε* and RNG *k-ε.* As seen in Table 3, the SST model computed the most comparable results for the shell pressure drop and overall HT coefficient with experimental data, while the RNG *k-ε* model computed the best results for the pressure drop in tubes. Based on all three categories, the chosen model for further computation was the SST turbulence model.

Further simulations were done for Reynolds numbers ranging from $9.2 \cdot 10^4$ to $15.2 \cdot 10^4$ for the shell and from $2.16 \cdot 10^4$ to $3.6 \cdot 10^4$ for tubes. As presented in Table 5 and seen in Figure 5, the pressure drop in the shell is under-predicted by SW with a deviation of 16–22%, whereas the pressure drop in tubes is over-predicted by approximately 4%. In Ansys CFX, the pressure drop in the shell is under-predicted with a deviation of 1-6%. The deviation in tubes is over-predicted between 14 and 17%. Generally, Ansys CFX better predicts the pressure drop in the shell by 16%, while SW computed better results for the tube pressure drop by about 11%.

The overall HT coefficient was also simulated for all above mentioned Reynolds numbers, as seen in Table 7 and Figure 6. SWFS under-predicts the result by approximately 9%. In Ansys CFX, the SST turbulence model under-predicted the overall HT coefficient with a deviation of 1–6%. In general, Ansys CFX better predicts the overall HT coefficient by 4–8%.

Based on the computed results of the pressure drops and the overall HT coefficient, the Ansys SST turbulence model would be the better choice for the example used in this paper. Nevertheless, if we take into account the time and effort to make a structured mesh in ICEM CFD, SWFS would be sufficient for this CFD problem since the results are comparable.

References

[1] **U. U. Rehman:** *Heat Transfer Optimization of Shell-and-Tube Heat Exchanger through CFD Studies*, Master's Thesis, Chalmers University of Technology, Department of Chemical and Biological Engineering, 2011

Available at: http://publications.lib.chalmers.se/records/fulltext/155992.pdf,

Accessed on December 13, 2014

[2] **H. Kotwal, S. Patel:** *CFD Analysis of Shell and Tube Heat Exchanger - A Review*, International Journal of Engineering Science and Innovative Technology (IJESIT), Volume 2, Issue 2, 2013

Available at: http://www.ijesit.com/Volume%202/Issue%202/IJESIT201302_49.pdf,

Accessed on December 13, 2014

[3] **A. Sobachkin, G. Dumnov:** *Numerical Basis of CAD-Embedded CFD,* 2014

Available at: http://www.solidworks.com/sw/docs/Flow_Basis_of_CAD_Embedded_CFD_Whitepaper.pdf, Accessed on October 6, 2014